Approaches to eliminate near field artifact of MURA

WANG Ren-Song(王人松) RONG Jun-Yan(戎军艳) WEI Long(魏龙)[1)]

(Key Laboratory of Nuclear Analysis Techniques, Institute of High Energy Physics, CAS, Beijing 100049, China)

Abstract Since the coded aperture technique has been successfully applied on X-ray imaging space telescopes, attentions of its development have also been cast on the application in medical imaging, for it has a very tempting quality to greatly enhance the detection sensitivity without gravely lowering the spacial resolution. But when the coded aperture technique is applied to image a nearby object, the so called "near-field artifact" comes up, that is, the reconstructed image has a sort of distortion. Among types of coded apertures the MURA (Modified Uniformly Redundant Array) is one of the most discussed. Roberto Arrcosi came up with the solution to remove the artifacts utilizing mask and antimask. In this article we present two ways to eliminate the second order aberration based on his work.

Key words MURA, coded aperture, MLEM, optical supplementary principle

PACS 42.30.Lr, 42.30.Va, 42.30.Wb

1 Introduction

The application of coded aperture imaging in clinical use as well as others like the verification of radioactive contamination[1, 2], is currently a hotspot in radioactive imaging research. And the Modified Uniformly Redundant Aperture[3] (MURA) is recognized as an optimal solution[4] up to now. Within the applications of MURA the technique developed by Roberto Arrcosi[5] has been proved effective in cancellation of the near field aberration caused by $\cos^3\theta$ (θ denotes the incident angle) modulation with mask and antimask. But it requires two measures to get one image, and in practical use one must double either the measure time or the cost of instrument manufacturing. In this paper we focus on the near field planar object imaging and present two ways to cancel the first and second order aberration of $\cos^3\theta$ in one measure. One is the well known maximum likelihood expectation maximization (MLEM)[6, 7], and the other is based on optical supplementary principle.

2 MLEM simulation

The idea of utilizing the MLEM algorithm comes naturally after the work of the Synthetic Collimator[8—10]. There they used multi-pinhole aperture and achieved good results in discerning point source three dimensionally. While in our case, the mask is half open, so the probability matrix, which indicates the likelihood of each source point detected by each detector, is not an sparse matrix. More than half of its elements are not zero. So that takes up a lot of memory space. Here we assume that the radioactive object is within a plane parallel to the mask and detector planes, also the mask aperture and the scintillator detectors are ideal. The mask is a 11×11 mosaicked MURA, with unit length of each pixel, that is, the whole mask is 22×22 in length. And the detector array is composed of 22×22 scintillator crystals of the same unit pixel size. The distances from the source plane to the mask, and the mask to the detector, are both 10, so one can see that it is indeed a very near measurement. Both the approaches mentioned in the article apply the delta decoding technique[11]. Left of Fig. 1 is the planar object of "OK" we used in our simulation. It has in total 88×88 pixels, i.e. each 4×4 pixels' average should be acquired by our reconstructed image in an ideal far field case. The middle one is the direct decoding image we get using common cyclic correlation method (delta as well). The right one is the decoded image after 25 iterations of MLEM with an uniform start. We can see that there are no "bows" compared with the direct decoding one.

But from the simulation we find that MLEM gets

Received 22 December 2006, Revised 3 September 2007

1) E-mail: weil@ihep.ac.cn

its own problems. The first problem is its huge consumption of computer resources, as is commonly known. In our case the simplified probability matrix we used in the simulation is 4 dimensional with each dimensional length being 22, i.e., it contains totally $22^4 = 234256$ data in double float format and occupies about 1.8 MB memory. And it takes 5.9 s to go though all 25 iterations on a Pentium 2.0 GHz PC. Since it scales 4 powers of exponent as the image length and takes a long time to compute, we may doubt its practical application. The second is that, apart from its computation limitation, there are still some artifacts produced by MLEM. For instance the upper right bar of the letter "K" has an unproper and fuzzy extension, and it is most likely to relate with the shape of the object itself. Additionally the image contrast has decreased compared to the direct decoding one. Therefore we present an alternative way to approximately cancel the artifact without burdening computers so heavily.

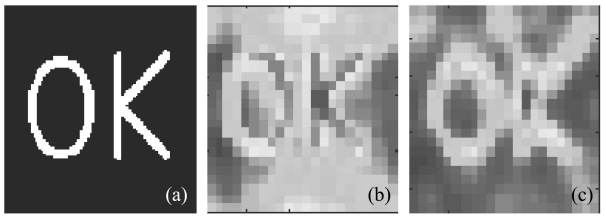

Fig. 1. The radioactive object (a), reconstructed image by a 11×11 mosaicked MURA using direct decoding (b), reconstructed image using MLEM (c).

3 Optical supplementary principle

To compare with the above result, here we do not change any of that optical system. As a common definition, A and G stand for the mask aperture and the decoding pattern separately. And (1-A ,-G) are the antimask and the corresponding decoding pattern. If you add mask and antimask together, you will get a total transparent aperture, if the original mask border is not considered. Therefore we can use a totally transparent aperture to replace the antimask measurement. Then we subtract the first measurement readout from this one and get the antimask readout as it is the optical supplementary principle. In fact we have found such such a thing interesting.

Figure 2 is Acorrsi's mask-antimask procedure: a is the reconstructed image of mask and b is the one of antimask, (c) is the summation of the two figures (i.e., (a)+(b)) and (d) is (a)−(b). We see that Fig. (c) cancels artifacts and reinforces the reconstruction, and that Fig. (d) cancels the object and reinforces the artifacts. Fig. 3(a) is the decoded image with no aperture (i.e. the total transparency aperture) placed between the object and the detector, and Fig. 3(b) is the reconstructed image of 3(a). We can hardly see the differences between Fig. 3(b) and 2(d) except the difference in intensity.

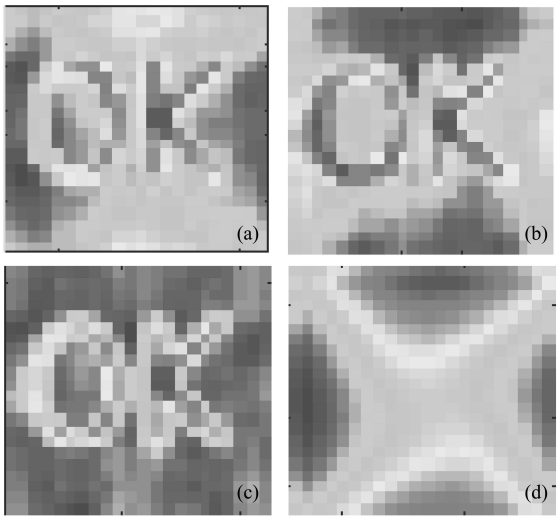

Fig. 2. (a) The reconstructed image obtained by the same 11×11 mask; (b) The image obtained by the antimask of (a); (c) The sum of pictures (a) and (b); (d) The difference of (a) and (b).

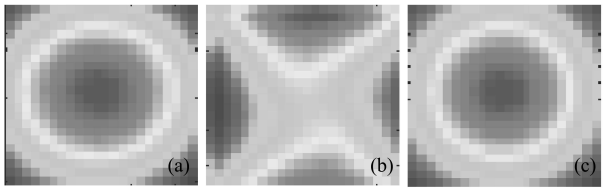

Fig. 3. (a) The detector image of the object "OK" with no aperture; (b) The reconstructed image of (a); (c) The detector image of a point source with no aperture.

The derivation of the formula is very simple. Eq. (1) is the one in Ref. [5]

$$\hat{O} \propto \left\{ \iint_{\xi} O'(\xi) A'(r_{\mathrm{i}} - \xi) \cos^3 \times \left[\arctan\left(\frac{|r_{\mathrm{i}} + (a/b)\xi|}{z} \right) \right] \mathrm{d}^2\xi \right\} \otimes G = \left\{ \iint_{\xi} O'(\xi) A'(r_{\mathrm{i}} - \xi) \cos^3 \theta_{\xi} \mathrm{d}^2\xi \right\} \otimes G \,. \quad (1)$$

Here $\hat{O}$ is the reconstructed image, O' and A' are respectively the rescaled and reflected form of the object and the rescaled projection of the mask. G denotes the decoding pattern. While in the case of antimask, $\hat{O}$ becomes

$$\hat{O}_a \propto \left\{ \iint_{\xi} O'(\xi) [1 - A'(r_{\mathrm{i}} - \xi)] \cos^3 \theta_{\xi} \mathrm{d}^2\xi \right\} \otimes (-G) \,. \quad (2)$$

Now if we subtract Eq. (2) from (1) we get

$$\hat{O}_{\rm s} := \hat{O} - \hat{O}_a \propto \left\{ \iint_{\xi} O'(\xi) \cos^3\theta_{\xi} {\rm d}^2\xi \right\} \otimes G\,. \qquad (3)$$

Obviously $\hat{O}_{\rm s}$ is an image reconstructed without the mask. So we can just replace the antimask measurement with one without mask, and subtract from it the first measurement in order to get an antimask readout.

On second thoughts, we may conclude that the $\cos^3\theta$ effect maintains even without the aperture. And the total transparent aperture effectively effaces the shape of the object, that is, the detector readout is insensitive to the source distribution. Furthermore, we can replace in simulation the no aperture measurement with a simple point source that has the total intensity and the centre of mass of the first reconstructed "OK". In this way we get Fig. 3(c). And this "second measurement" can thoroughly be stored in the computer. Fig. 4 is what we get under these considerations, that is, the detector readout of the antimask is generated in simulation with Fig. 3(c) - Fig. 2(a), the 1st and 2nd order aberrations are also eliminated approximately.

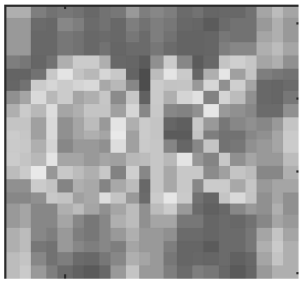

Fig. 4. The near field artifacts canceled in one measurement.

4 Conclusion and further work

We have found a way to approximately cancel the 1st and 2nd order aberrations caused by $\cos^3\theta$ near field effect in one measurement without immoderate requirement of the computing ability. The application of this skill may lie on the clinical planar imaging such as thyroid, etc. There we may use a common shaped phantom of the thyroid to replace the point dot referred above to further improve the final image in simulation. A practical experiment is to be carried out to verify the algorithm.

References

1 Gal O, Gmar M, Ivanov O P et al. Nucl. Instrum. Methods, **A**, to be published
2 Woodring M, Beddingfield D, Souza D et al. Nucl. Instrum. Methods, 2003, **A505**: 415—419
3 Gottesman S R, Fenimore E E. Appl. Opt., 1989, **28**: 4344
4 Accorsi R, Gasparini F, Lanza R C. Nucl. Instrum. Methods, 2001, **A474**: 273—284
5 Accorsi R, Lanza R C. Appl. Opt., 2001, **40**: 4697—4705
6 Shepp L, Vardi Y. IEEE Trans. Med. Imag., 1982, **1**: 113—122
7 Parra L, Barrett H H. IEEE Trans. Med. Imag., 1998, **17**(2): 228—235
8 Wilson D W, Barrett H H, Clarkson E W. IEEE Trans. Med. Imag., 2000, **19**(5): 412—422
9 Clarkson E, Barrett H H, Wilson D W. Proc. SPIE, 1998, **3336**: 251—259
10 Clarkson E, Wilson D W, Barrett H H. Proc. SPIE, 1999, **3659**: 107—117
11 Fenimore E E, Cannon T M. Appl. Opt., 1981, **20**: 1858—1864